

Fast Two-Stage Variational Bayesian Approach to Estimating Panel Spatial Autoregressive Models with Unrestricted Spatial Weights Matrices

Deborah Gefang¹, Stephen G. Hall², and George S. Tavlas³

¹University of Leicester

²University of Leicester, Bank of Greece and University of Pretoria

³Bank of Greece and Hoover Institution, Stanford University

Abstract

This paper proposes a fast two-stage variational Bayesian algorithm to estimating panel spatial autoregressive models with unknown spatial weights matrices. Using Dirichlet-Laplace global-local shrinkage priors, we are able to uncover the spatial impacts between cross-sectional units without imposing any a priori restrictions. Monte Carlo experiments show that our approach works well for both long and short panels. We are also the first in the literature to develop VB methods to estimate large covariance matrices with unrestricted sparsity patterns, which is useful for other popular large data models such as Bayesian vector autoregressions. In empirical applications, we examine the relationships between euro area sovereign bond ratings and sovereign spreads using rolling window estimations. Our findings indicate marked differences between the spillover behaviours of the northern euro area countries and that of the south.

JEL Classification: C11; C33; C55

Keywords: Variational Inference; Spatial Panel Data Models; Simultaneous Equations; Large Data

1 Introduction

The spatial autoregressive (SAR) models, first proposed by Cliff and Ord (1973), have been widely used in the literature to investigate the spatial dependence in cross-sectional units (e.g., Anselin, 1988; Baltagi et al., 2003, 2013; Lee and Yu, 2010). In practice, the spatial weights matrices are usually set a priori based on geographical distances or economic characters (e.g. Cliff and Ord, 1973; Anselin, 1988; Case, 1991). This is not surprising as a spatial weights matrix potentially involves $N^2 - N$ interrelationships between N spatial units, which makes it difficult to estimate, especially when N is large.

In recent years, a number of variable selection and parameter shrinkage methods have been developed to estimate the spatial weights matrices of panel SAR models. Among them, methods resorting to least absolute shrinkage and selection operator (Lasso) of Tibshirani’s (1996) and its variants have gained a lot of attention. For example, Basak et al. (2018) propose to estimate a triangular weights matrix under the assumption of recursive ordering. Ahrens and Bhattacharjee (2015) develop a two step Lasso estimator to identify the weights matrix. Lam and Souza (2019) estimate the weights matrix using adaptive Lasso with sparse adjustment in mind. Most of the studies, however, usually impose sometime unrealistic restrictions on the model’s coefficients or covariances. Krock et al. (2021) develop a graphical Lasso approach to estimating the unrestricted covariances. Their method, however, does not deal with the impacts of any possible exogenous variables. Moreover, to our knowledge, few of those studies focus on the short panels where N is large while T is small.

This paper contributes to the SAR literature by developing a fast two-stage variational Bayesian (VB) approach to estimating panel SAR models with unknown spatial weights matrices. We do not impose any restrictions on spatial weights matrix or the covariance functions, hence our approach lets the data speak. The prior we used for Bayesian regularization is the Dirichlet–Laplace (D–L) prior of Bhattacharya et al. (2015). With D–L prior, the entire posterior distribution concentrates at the optimal rate. This nice feature remains unchanged when the number of parameters to be estimated is much larger than the number of observations, providing strong theoretical justifications for the two-stage VB’s effectiveness in uncovering the spatial dependencies in a short panel.

A secondary contribution of this paper lies in developing VB methods for estimating large covariance matrices with D-L prior. We are among the first in the literature to develop VB estimator for large covariance matrices with unknown sparsity patterns. Our VB methods using D-L prior can be easily extended to allow for other popular priors such as the graphic Lasso of Wang (2012), the half-Cauchy prior of Makalic and Schmidt (2016) and the graphical horseshoe prior of Li et al. (2019). This is not trivial as VB is a more computationally efficient alternative of Markov Chain Monte Carlo (MCMC), and our approach can be used in estimating other popular models involving large covariance matrices such as large Bayesian vector autoregressions (BVARs).¹

We have conducted a wide range of simulation studies using a traditional panel SAR model and a panel SAR model that takes account of the simultaneous relationships between cross-sectional groups.² Monte Carlo experiments show that two-stage VB is accurate and computationally efficient when $T \gg N$, which usually is more pertinent to macroeconomic and financial data. When $N \gg T$, which tends to be more relevant to microeconomic data, two-stage VB estimates tend to have slightly larger biases and empirical standard deviations. Tighter priors can help lessen that problem.

In empirical applications, we use two-stage VB to estimate a two-equation simultaneous spatial model using panel data comprising sovereign bond ratings and spreads of ten eurozone countries. The research is motivated by the importance of a more in-depth understanding in how cross-country contagion works in the southern euro area countries and their northern counterparts, especially in the European debt crises (e.g. Gibson et al., 2021; Hall et al., *forthcoming*). Using rolling windows of 2, 3, 5 and 10 years, respectively, we compare and contrast how the spillovers of the south and the north affect each individual member country. Our results provide ample evidence for the marked differences between the two country groups, both in how spillovers of the south and the north impact a country in a very different way and in how spillovers of a particular country group affect a southern and a northern country very differently. Our results also highlight the big impacts of the global financial crises and how the south was severely affected by the European debt crises while the north was much

¹Matlab code is provided.

²This research used the ALICE High Performance Computing Facility at the University of Leicester.

less so.

The rest of the paper is organised as follows. Section 2 extends the traditional panel SAR models to an unrestricted panel SAR. Section 3 develops the two-stage VB. Section 4 conducts Monte Carlo studies. Section 5 applies two-stage VB to the sovereign bond ratings and spreads data of ten euro area countries. Section 6 concludes. Sources for data used in the empirical example are listed in the Appendix. Detailed VB derivation formulas and more extensive Monte Carlo results are relegated to On-line Appendices A to C.³

In this section, we start from a traditional standard panel SAR and then relax the restrictions imposed upon it in steps, with the aim of giving a flavour of the differences between the traditional model and the unrestricted panel SAR model that we set to estimate using two-stage VB.

Let Y , X and V denote the $T \times N$ matrix of endogenous variables, $T \times (Nm)$ matrix of exogenous variables, and $T \times N$ matrix of disturbances, respectively. A traditional panel SAR model takes the following form:

$$y_t = \lambda W_n y_t + X_t \beta + u_t, \quad |\lambda| < 1 \quad (1)$$

where $y_t = (Y_{t1}, Y_{t2}, \dots, Y_{tN})'$ is the $N \times 1$ vector of observations of the dependent variables, W_n is an $N \times N$ known spatial weights matrix with zero diagonal

entries, $X_t = \begin{pmatrix} X_{t,1} \\ X_{t,2} \\ \dots \\ X_{t,N} \end{pmatrix}$ is the $N \times m$ matrix of exogenous variables, with $X_{t,i}$

denoting the $1 \times m$ row vector of exogenous variables associated with dependent variable y_{ti} , β is an $m \times 1$ vector of parameters, λ is a scalar parameter, and $u_t = (V_{t1}, V_{t2}, \dots, V_{tN})'$ is the $N \times 1$ i.i.d error terms with mean zero and diagonal

covariance matrix $\begin{pmatrix} \sigma^2 & 0 & \dots & 0 \\ 0 & \sigma^2 & \dots & 0 \\ \dots & \dots & \dots & \dots \\ 0 & 0 & \dots & \sigma^2 \end{pmatrix}$.

³The online appendices are available at <https://github.com/DBayesian/GKT2022>

Model (1) imposes the following unrealistic restrictions on the data generating process:

- 1) W_N is predetermined, in a fashion that is not related to the variations in the data;
- 2) λ and β remain the same across equations associated with different dependent variables; and
- 3) the covariance matrix of u_t is diagonal with the same diagonal entries.

Relaxing those restrictions, model (1) can be written as:

$$y_t = \tilde{\lambda} \odot (\widetilde{W}_N y_t) + \widetilde{X}_t \tilde{\beta} + u_t, \quad |\lambda_b|_\infty < 1 \quad (2)$$

where \widetilde{W}_N is an $N \times N$ unknown spatial weight matrix with zero diagonal entries, $\tilde{\lambda}$ is a

$$N \times 1 \text{ parameter vector, } \odot \text{ is the Hadamard product, } \widetilde{X}_t = \begin{pmatrix} X_{t,1} & 0 & \dots & 0 \\ 0 & X_{t,2} & \dots & 0 \\ \dots & \dots & \dots & \dots \\ 0 & 0 & \dots & X_{t,N} \end{pmatrix},$$

$\tilde{\beta}$ is a $Nm \times 1$ parameter vector, and u_t is i.i.d with mean zero and diagonal covariance matrix $\tilde{\Sigma}$ with diagonal entries that can be different from each other. In this model, the dimensions of $X_{t,i}$ and $X_{t,j}$ for $i \neq j$ can differ from each other. Let the dimension of $X_{t,i}$ to be $1 \times m_i$. The dimension of the parameter vector $\tilde{\beta}$ is thus $(\sum_{i=1}^n m_i) \times 1$.

Note that model (2) is quite flexible. For example, with appropriate restrictions, it can be easily transformed back into the traditional form described in (1) or a panel SAR containing the simultaneous cross-sectional spatial relationship as described in Yang and Lee (2017) and Liu and Saraiva (2019).

Since our main concerns in panel SAR models are the spillover effects, there is therefore little research interest in separately identifying $\tilde{\lambda}$ and \widetilde{W}_N . What we care about is the product $(\tilde{\lambda} \otimes l_N) \odot \widetilde{W}_N$, where l_N is a $N \times 1$ column of ones and \otimes is the Kronecker product, as $(\tilde{\lambda} \otimes l_N) \odot \widetilde{W}_N$ is the $N \times N$ parameter matrix which captures the spillover effects between spatial units.

Let $\Lambda = (\tilde{\lambda} \otimes l_N) \odot \widetilde{W}_N$. Model (2) can be written as:

$$y_t = \Lambda y_t + \widetilde{X}_t \tilde{\beta} + u_t, \quad (3)$$

where $I_N - \Lambda$ is nonsingular and the characteristic roots of $I_N - \Lambda$ lie within the unit circle.

The attractiveness of model (3) is that it turns an unrestricted panel SAR model into a system of simultaneous equations (SEM). As shown in Zellner and Thell (1962) and Fox (1979), the i^{th} equation in model (3) is just identified if $\sum_{i=1}^N m_i = N - 1 + m_i$ and over-identified if $\sum_{i=1}^N m_i > N - 1 + m_i$. Under these circumstances, a myriad of estimation methods, such as two-stage least squares (2SLS), three-stage least squares (3SLS), maximum likelihoods methods and simultaneous generalized method (GMM), can be used to uncover the structural parameters Λ and $\tilde{\beta}$. Moreover, standard tests can be developed to test the restrictions on $\tilde{\lambda}$, \tilde{W}_N and $\tilde{\beta}$, if those restrictions are of the researchers' concerns.

This paper proposes to estimate Λ and $\tilde{\beta}$ in two stages as it is computationally simple. To estimate the parameters associated with the i^{th} individual dependent variable, in the first stage, we estimate

$$Y_{/i} = X\Upsilon_i + E_i, \quad (4)$$

where $Y_{/i}$ is the $T \times (N - 1)$ matrix of dependent variables except for the i^{th} dependent variable, and E_i is a $T \times (N - 1)$ matrix of error terms whose precision matrix might not be diagonal.

Making use of the estimated Υ_i , in the second stage, we estimate

$$y_i = \hat{Y}_{/i}(\Lambda_{i\bullet})' + X_{\bullet,i}\tilde{\beta}_i + u_i, \quad (5)$$

where y_i is the $T \times 1$ vector of the i^{th} dependent variable, $\hat{Y}_{/i} = X\Upsilon_i$, $\Lambda_{i\bullet}$ is the $1 \times (n - 1)$ vector of the i^{th} row of Λ with Λ_{ii} dropped, and $\tilde{\beta}_i$ is the corresponding coefficients in $\tilde{\beta}$.

Note that in a panel SAR model, we can have $N \gg T$ and $(N - 1 + m_i) \gg T$, which makes it difficult or even impossible to uncover B_i and $\Lambda_{i\bullet}$ using traditional estimation techniques.

2 Two-stage VB

As detailed in Ormerod and Wand (2010) and Blei et al. (2017), the essence of VB is to use appropriate densities from a mean field variational family to approximate the posterior densities through minimizing the Kullback-Leibler divergence, which is equivalent to maximising the evidence lower bound (ELBO). As a more efficient alternative to MCMC, VB has been increasingly used in sophisticated models involving large data where MCMC is too computationally expensive or even untenable (e.g. Gefang et al., 2020, 2022; Loaiza-Maya et al., 2022).

In the two-stage VB, we identify the parameters in model (3) equation by equation. In each stage, we update the parameters using the approximate q densities by iterations. The convergence of the algorithm can be measured by the changes in ELBO across iterations is less than a convergence criteria. When the number of parameters is large, however, calculating ELBO can be time consuming. It is therefore more convenient to check if convergence has occurred by examining if the VB estimates of parameters stop changing across iterations.

2.1 First-stage VB

In the first stage, we estimate model (4) in order to construct the predicted value of $Y_{/i}$.

Let $\gamma = \text{vec}(\Upsilon_i)$. We set hierarchical D-L prior for the j^{th} , for $j = 1, \dots, np$, element of γ as follows:

$$\gamma_j | \phi, \tau \sim DE(\phi_j \tau), \quad \phi_j \sim Dir(a, \dots, a), \quad \tau \sim G(npa, 1/2). \quad (6)$$

where $DE(\bullet)$ denotes Double Exponential or Laplace distribution, $Dir(\bullet)$ denotes Dirichlet distribution, $G(\bullet)$ denotes Gamma distribution, $n = N - 1$, and $p = \sum_{i=1}^N m_i$.

Next, we set Exponential priors and D-L priors for the elements of Ω , the precision

matrix of E_i , as follows:

$$\begin{aligned} \omega_{ii} &\sim \text{Exp}(\underline{s}), \quad i = 1, \dots, n \\ \omega_{ij} &\sim N(0, \psi_{\omega,ij} \phi_{\omega,ij}^2 \tau_{\omega}^2), \quad \psi_{\omega,ij} \sim \text{Exp}(1/2), \quad i < j = 2, \dots, n, \\ \phi_{\omega,ij} &\sim \text{Dir}(a_{\omega}, \dots, a_{\omega}), \quad \tau_{\omega} \sim G(\frac{n^2 - n}{2} a_{\omega}, 1/2) \end{aligned} \quad (7)$$

where, with a slight abuse of notations, we use ω_{ii} and ω_{ij} to denote the diagonal and off-diagonal elements of Ω .

Following Wang's (2012) Block Gibbs sampler to update the relevant parameters and hyperparameters, we use the last column and row of Ω as an example on how to update Ω .

Let $S = E_i' E_i$ and H be the $n \times n$ matrix with 0 diagonal elements and the off diagonal element at i^{th} row and j^{th} column be $\psi_{\omega,ij} \phi_{\omega,ij}^2 \tau_{\omega}^2$. Partition Ω , S and H as follows:

$$\Omega = \begin{pmatrix} \Omega_{-n,-n} & \omega_{-n,n} \\ \omega'_{-n,n} & \omega_{nn} \end{pmatrix} \quad S = \begin{pmatrix} S_{-n,-n} & s_{-n,n} \\ s'_{-n,n} & s_{nn} \end{pmatrix} \quad H = \begin{pmatrix} H_{-n,-n} & h_{-n,n} \\ h'_{-n,n} & h_{nn} \end{pmatrix} \quad (8)$$

where $-n$ denotes the set of all indices except for n .

Relegating technical details to Online Appendix A, we outline the VB approximation densities as follows:

2.1.1 $q(\gamma)$

$$q(\gamma) \sim N(\bar{\gamma}, \bar{V}), \quad (9)$$

where

$$\bar{V} = (V^{-1} + \bar{\Omega} \otimes (X'X))^{-1},$$

$$\bar{\gamma} = \bar{V}(\bar{\Omega} \otimes X') \text{vec}(Y_{/i}),$$

and

$$V^{-1} = \text{diag}(\frac{1}{\psi_1 \phi_1^2 \tau^2}, \dots, \frac{1}{\psi_{np} \phi_{np}^2 \tau^2})$$

2.1.2 $q(\tau)$

$$q(\tau) \sim giG[npa - np, 1, \sum_{j=1}^{np} 2(\bar{\gamma}_j^2 + \bar{V}_{jj})^{1/2} \frac{1}{\phi_j}], \quad (10)$$

Let $\chi = \sum_{j=1}^{np} 2(\bar{b}_j^2 + \bar{V}_{jj})^{1/2} \frac{1}{\phi_j}$, we have

$$\bar{\tau} = \frac{\sqrt{\chi} K_{npa-np+1}(\sqrt{\chi})}{K_{npa-np}(\sqrt{\chi})}$$

$$\bar{\tau}^2 = \bar{\tau}^2 + \chi \left[\frac{K_{npa-np+2}(\sqrt{\chi})}{K_{npa-np}(\sqrt{\chi})} - \left(\frac{K_{npa-np+1}(\sqrt{\chi})}{K_{npa-np}(\sqrt{\chi})} \right)^2 \right]$$

where $K_*[\bullet]$ is the modified Bessel functions of the second kind.

2.1.3 $q(\psi_j)$

$$q(\psi_j^{-1}) \sim iG\left(\sqrt{\frac{\bar{\phi}_j^2 \bar{\tau}^2}{\bar{\gamma}_j^2 + \bar{V}_{jj}}}, 1\right), \quad (11)$$

where $iG(\bullet)$ denotes s Inverse Gaussian distribution.

$$\text{Let } \rho = \sqrt{\frac{\bar{\phi}_j^2 \bar{\tau}^2}{\bar{\gamma}_j^2 + \bar{V}_{jj}}},$$

$$\bar{\psi}_j^{-1} = \rho$$

and

$$\bar{\psi}_j = 1 + 1/\rho$$

2.1.4 $q(\phi_j)$

$$q(\xi_j) \sim giG(a - 1, 1, 2\sqrt{\bar{\gamma}_j^2 + \bar{V}_{jj}}), \quad (12)$$

where $giG(\bullet)$ denotes the generalized inverse Gaussian distribution.

Let $\varpi = 2\sqrt{\bar{\gamma}_j^2 + \bar{V}_{jj}}$, we have

$$\bar{\xi}_j = \frac{\sqrt{\varpi} K_a(\sqrt{\varpi})}{K_{a-1}(\sqrt{\varpi})},$$

and

$$\text{var}(\xi_j) = \varpi \left\{ \frac{K_{a+1}(\sqrt{\varpi})}{K_{a-1}(\sqrt{\varpi})} - \left[\frac{K_a(\sqrt{\varpi})}{K_{a-1}(\sqrt{\varpi})} \right]^2 \right\},$$

where $\text{var}(\bullet)$ denotes the variance.

Scaling ξ_i , we have

$$\overline{\phi_j} = \frac{\overline{\xi_j}}{\sum_{j=1}^{np} \overline{\xi_j}},$$

and

$$\overline{\phi_j^2} = \overline{\phi_j}^2 + \frac{\text{var}(\xi_j)}{(\sum_{j=1}^{np} \overline{\xi_j})^2}$$

Thus, the optimal q density of $\phi_{i,j}$ takes the following form:

$$q(\phi_j) \sim giG(a-1, \sum_{j=1}^{np} \overline{\xi_j}, \frac{2\sqrt{\overline{\gamma_j^2} + (\overline{V_{jj}})^2}}{\sum_{j=1}^{np} \overline{\xi_j}}) \quad (13)$$

2.1.5 $q(b_1)$

Let $b_1 = \omega_{n,n} - \omega'_{-n,n} \Omega_{-n,-n}^{-1} \omega_{-n,n}$.

$$q(b_1) \sim G\left(\frac{T}{2}, \overline{s}_{n,n}\right), \quad (14)$$

where

$$\overline{s}_{n,n} = \frac{1}{2}(s_{n,n} + \text{tr}(X'X\overline{V}_n) + \underline{s}),$$

and

$$\overline{V}_n = V_{(n-1) \times p+1:n \times p, (n-1) \times p+1:n \times p}.$$

Hence

$$\overline{b_1} = \frac{\frac{T}{2}}{\overline{s}_{n,n}}$$

2.1.6 $q(b_2)$

Here we use b_2 to denote $\omega_{-n,n}$. Let $\bar{s}_{-n,n} = s_{-n,n} + \tilde{s}_{-n,n}$, where $\tilde{s}_{-n,n}$ is a $(n-1) \times 1$ vector with the j^{th} element being $tr(X'XA_j)$ and $A_j = V_{(j-1) \times p+1:j \times p, (j-1) \times p+1:j \times p}$.⁴

$$q(b_2) \sim N(-\bar{C}\bar{s}_{-n,n}, \bar{C}), \quad (15)$$

where

$$\bar{C} = (2\bar{s}_{n,n}\Omega_{-n,-n}^{-1} + \bar{H}^{*-1})^{-1},$$

and

$$\bar{b}_2 = (-\bar{C}\bar{s}_{-n,n}).$$

Note that $\bar{H}^* = diag(\bar{h}_{-n,n})$, and j^{th} element of $\bar{h}_{-n,n}$ is $\overline{\psi_{\omega,jn}\phi_{\omega,jn}^2\tau_{\omega}^2}$.

2.1.7 $q(\tau_{\omega})$

$$q(\tau_{\omega}) \sim giG[\frac{n^2-n}{2}(a_{\omega}-1), 1, \sum_{j < k} 2(\overline{\omega_{jk}}^2 + \bar{C}_{jj})^{1/2} \frac{1}{\overline{\phi_{\omega,jk}}}],^5 \quad (16)$$

Let $\chi_{\omega} = \sum_{j < k} 2(\overline{\omega_{jk}}^2 + \bar{V}_{jj})^{1/2}(\overline{\phi_{\omega,jk}})^{-1}$, we have

$$\bar{\tau}_{\omega} = \frac{\sqrt{\chi_{\omega}} K_{\frac{n^2-n}{2}(a_{\omega}-1)+1}(\sqrt{\chi_{\omega}})}{K_{\frac{n^2-n}{2}(a_{\omega}-1)}(\sqrt{\chi_{\omega}})}$$

$$\bar{\tau}_{\omega}^2 = \bar{\tau}_{\omega}^{-2} + \chi_{\omega} \left[\frac{K_{\frac{n^2-n}{2}(a_{\omega}-1)+2}(\sqrt{\chi})}{K_{\frac{n^2-n}{2}(a_{\omega}-1)}(\sqrt{\chi_{\omega}})} - \left(\frac{K_{\frac{n^2-n}{2}(a_{\omega}-1)+1}(\sqrt{\chi_{\omega}})}{K_{\frac{n^2-n}{2}(a_{\omega}-1)}(\sqrt{\chi_{\omega}})} \right)^2 \right]$$

2.1.8 $q(\psi_{\omega,jn})$

$$q(\psi_{\omega,jn}^{-1}) \sim iG\left(\sqrt{\frac{\overline{\phi_{\omega,jn}^2\tau_{\omega}^2}}{\overline{\omega_{jn}^2} + \bar{C}_{jj}}}, 1\right), \quad (17)$$

⁴To calculate $\bar{s}_{-i,i}$, for $i \neq n$, we need to delete the relevant $(i-1) \times p+1$ to $i \times p$ rows and $(i-1) \times p+1$ to $i \times p$ columns of \bar{V} to construct A_j .

⁵Note that \bar{C}_{jj} changes when k changes.

Let $\rho_\omega = \sqrt{\frac{\phi_{\omega,jn}^2 \tau_\omega^2}{\omega_{jn}^{-2} + \overline{C}_{jj}}}$,

$$\overline{\psi_{\omega,jn}^{-1}} = \rho_\omega$$

and

$$\overline{\psi_{w,jn}} = 1 + 1/\rho_\omega$$

2.1.9 $q(\phi_{\omega,jn})$

$$q(\xi_{\omega,jn}) \sim giG(a_\omega - 1, 1, 2\sqrt{\omega_{jn}^{-2} + \overline{C}_{jj}}) \quad (18)$$

Let $\varpi_\omega = 2\sqrt{\omega_{jn}^{-2} + \overline{C}_{jj}}$, we have

$$\overline{\xi_{\omega,jn}} = \frac{\sqrt{\varpi_\omega} K_{a_\omega}(\sqrt{\varpi_\omega})}{K_{a_\omega-1}(\sqrt{\varpi_\omega})},$$

and

$$var(\xi_{\omega,jn}) = \varpi_\omega \left\{ \frac{K_{a_\omega+1}(\sqrt{\varpi_\omega})}{K_{a_\omega-1}(\sqrt{\varpi_\omega})} - \left[\frac{K_{a_\omega}(\sqrt{\varpi_\omega})}{K_{a_\omega-1}(\sqrt{\varpi_\omega})} \right]^2 \right\},$$

where $var(\bullet)$ denotes the variance.

Scaling $\xi_{\omega,jn}$, we have

$$\overline{\phi_{\omega,jn}} = \frac{\overline{\xi_{\omega,jn}}}{\sum_{j < k} \overline{\xi_{\omega,jk}}},$$

and

$$\overline{\phi_{\omega,jn}^2} = \overline{\phi_{\omega,jn}}^2 + \frac{var(\xi_{\omega,jn})}{\left(\sum_{j < k} \overline{\xi_{\omega,jk}} \right)^2}$$

Thus, the optimal q density of $\phi_{\omega,ij}$ takes the following form:

$$q(\phi_{\omega,jn}) \sim giG(a - 1, \sum_{j < k} \overline{\xi_{\omega,jk}}, \frac{2\sqrt{\omega_{jn}^{-2} + (\overline{C}_{jj})^2}}{\sum_{j < k} \overline{\xi_{\omega,jk}}}) \quad (19)$$

2.2 Second-stage VB

We explain the technical details of second-stage VB in Online Appendix B. Below we briefly describe the priors of the parameters and hyperparameters and then provide their optimal q densities.

Let $Z = (\widehat{Y}_{/i} \ X_{\bullet,i})'$ and $\theta = [(\Lambda_{i\bullet})' \ \tilde{\beta}_i]$.

We elicit hierarchical D-L prior for θ as follows:

$$\theta_j | \tilde{\phi}, \tilde{\tau} \sim DE(\tilde{\phi}_j \tilde{\tau}), \quad \tilde{\phi}_j \sim Dir(\tilde{a}, \dots, \tilde{a}), \quad \tau \sim G(k\tilde{a}, 1/2) \quad (20)$$

where $k = N - 1 + m_i$.

Next we set a Gamma prior for σ^{-2} :

$$\sigma^{-2} \sim G(\nu, \tilde{S}). \quad (21)$$

The VB optimal densities can be found as follows:

2.2.1 $q(\theta)$

$$q(\theta) \sim N(\bar{\theta}, \bar{\tilde{V}}), \quad (22)$$

where

$$\begin{aligned} \bar{\tilde{V}} &= \left(\frac{T}{2} + \nu \right) \frac{Z'Z}{\bar{\tilde{S}}} + \tilde{V}^{-1} \\ \bar{\theta} &= \left(\frac{T}{2} + \nu \right) \frac{\tilde{V} Z' y_i}{\bar{\tilde{S}}} \\ \tilde{V}^{-1} &= diag(\bar{\psi}_1^{-1} \bar{\phi}_1^{-2} \bar{\tau}^{-2}, \dots, (\bar{\psi}_k^{-1} \bar{\phi}_k^{-2} \bar{\tau}^{-2})) \end{aligned}$$

2.2.2 $q(\sigma^{-2})$

$$q(\sigma^{-2}) \sim G\left(\frac{T}{2} + \nu, \bar{\tilde{S}}\right), \quad (23)$$

where

$$\bar{\tilde{S}} = \frac{1}{2} [||y_i - Z\bar{\theta}||^2 + tr(Z'Z\bar{\tilde{V}})] + \tilde{S}$$

2.2.3 $q(\tilde{\tau})$

$$q(\tilde{\tau}) \sim giG[k\tilde{a} - k, 1, \sum_{j=1}^k 2(\tilde{\theta}_j^2 + \tilde{V}_{jj})^{1/2} \frac{1}{\tilde{\phi}_j}], \quad (24)$$

Let $\tilde{\chi} = \sum_{j=1}^k 2(\tilde{\theta}_j^2 + \tilde{V}_{jj})^{1/2} \frac{1}{\tilde{\phi}_j}$, we have

$$\tilde{\tau} = \frac{\sqrt{\tilde{\chi}} K_{k\tilde{a}-k+1}(\sqrt{\tilde{\chi}})}{K_{k\tilde{a}-k}(\sqrt{\tilde{\chi}})}$$

and

$$\tilde{\tau}^2 = \tilde{\tau}^2 + \chi \left[\frac{K_{k\tilde{a}-k+2}(\sqrt{\tilde{\chi}})}{K_{k\tilde{a}-k}(\sqrt{\tilde{\chi}})} - \left(\frac{K_{k\tilde{a}-k+1}(\sqrt{\tilde{\chi}})}{K_{k\tilde{a}-k}(\sqrt{\tilde{\chi}})} \right)^2 \right]$$

2.2.4 $q(\tilde{\psi}_j)$

$$q\left(\frac{1}{\tilde{\psi}_j}\right) \sim iG\left(\sqrt{\frac{\tilde{\phi}_j^2 \tilde{\tau}^2}{\tilde{\theta}_j^2 + \tilde{V}^{jj}}}, 1\right), \quad (25)$$

$$\text{Let } \tilde{\rho} = \sqrt{\frac{\tilde{\phi}_j^2 \tilde{\tau}^2}{\tilde{\theta}_j^2 + \tilde{V}^{jj}}},$$

$$\frac{1}{\tilde{\psi}_j} = \tilde{\rho}$$

and

$$\tilde{\psi}_j = 1 + 1/\tilde{\rho}$$

2.2.5 $q(\tilde{\phi}_j)$

$$q(\tilde{\xi}_j) \sim giG(\tilde{a} - 1, 1, 2\sqrt{\tilde{\theta}_j^2 + (\tilde{V}_{jj})^2}) \quad (26)$$

Let $\tilde{\omega} = 2\sqrt{\tilde{\theta}_j^2 + (\tilde{V}_{jj})^2}$, we have

$$\tilde{\xi}_j = \frac{\sqrt{\tilde{\omega}} K_{\tilde{a}}(\sqrt{\tilde{\omega}})}{K_{\tilde{a}-1}(\sqrt{\tilde{\omega}})},$$

and

$$var(\tilde{\xi}_j) = \tilde{\omega} \left\{ \frac{K_{\tilde{a}+1}(\sqrt{\tilde{\omega}})}{K_{\tilde{a}-1}(\sqrt{\tilde{\omega}})} - \left[\frac{K_{\tilde{a}}(\sqrt{\tilde{\omega}})}{K_{\tilde{a}-1}(\sqrt{\tilde{\omega}})} \right]^2 \right\}.$$

Scaling $\tilde{\xi}$, we have

$$\bar{\tilde{\phi}}_j = \frac{\bar{\tilde{\xi}}_j}{\sum^k \bar{\tilde{\xi}}_j},$$

and

$$\bar{\tilde{\phi}}_j^2 = \bar{\tilde{\phi}}_j^2 + \frac{var(\tilde{\xi}_j)}{(\sum^k \bar{\tilde{\xi}}_j)^2}$$

Thus, the optimal q density of $\tilde{\phi}_j$ takes the following form:

$$q(\tilde{\phi}_j) \sim giG[\tilde{a} - 1, \sum^k \bar{\tilde{\xi}}_j, (2\sqrt{\bar{\theta}_j^2 + (\bar{V}_{jj})^2})/(\sum^k \bar{\tilde{\xi}}_j)] \quad (27)$$

3 Monte Carlo Studies

In the Monte Carlo studies, we look into two traditional panel SAR models of various sample sizes. The first model is:

$$y_t = 0.6W_N y_t + 0.9x_t + u_t, \quad (28)$$

where to specify W_N , we let each cross-sectional unit be connected with the unit ahead of it and the unit behind, and then normalize W by rows. When conducting Monte Carlo, we generate x_t and u_t independently from $N(0, 1)$ and $0.1N(0, 1)$, respectively.

The second model is:

$$\begin{aligned} y_{t,1} &= 0.5y_{t,2} + 0.6W_{N_1}y_{t,1} + 0.4W_{N_2}y_{t,2} + 0.9x_{t,1} + u_{t,1} \\ y_{t,2} &= 0.5y_{t,1} + 0.4W_{N_1}y_{t,1} + 0.6W_{N_2}y_{t,2} + 0.9x_{t,2} + u_{t,2} \end{aligned} \quad (29)$$

where $y_{t,1}$ is a vector of half of the N dependent variables observed at time t , and $y_{t,2}$ is the other half. When setting W_{N_1} and W_{N_2} , we assume a variable in $y_{t,1}$ is only

spatially related with the unit ahead of it and the unit behind, likewise a variable in $y_{t,2}$. Both W_{N_1} and W_{N_2} are normalized by rows. In Monte Carlo, we generate each element of $x_{t,1}$ and $x_{t,2}$ independently from $N(0, 1)$, then each element of $u_{t,1}$ and $u_{t,2}$ independently from $0.1N(0, 1)$.⁶

For both (28) and (29), the sample sizes considered are $N = 30$ and $T = 20$, $N = 30$ and $T = 80$, $N = 50$ and $T = 30$, $N = 50$ and $T = 100$, $N = 100$ and $T = 50$, and $N = 100$ and $T = 200$. For each case, we conduct 1000 Monte Carlo replications and use the changes in parameters instead of that of ELBO to check whether two-stage VB has converged.

Tables 1-2 report the Monte Carlo results of parameter Λ and $\tilde{\beta}$ for model (28) with $N = 30$ and $T = 80$ as well as $N = 30$ and $T = 20$. To save space, we only report the mean and standard deviations, the latter in parenthesis, of the empirical distributions of the first and last five rows of Λ , which are associated with $y_{t,1}, \dots, y_{t,5}$ and $y_{t,26}, \dots, y_{t,30}$ and relegate those of the other rows to the Online Appendix C.

Tables 3-4 report the Monte Carlo results of parameter Λ and $\tilde{\beta}$ for model (29) with $N = 30$. Again, we only include the first and last five rows of Λ , but all the elements in $\tilde{\beta}$, leaving the rest of Λ to Online Appendix C.

Results in Tables 1-4 provide strong evidence that the two-stage VB is able to recover the true parameters in the data generating process, especially when $T \gg N$. When $T \ll N$, two-stage VB estimates have larger biases and larger empirical standard deviations, which can be reduced by setting tighter priors. More important, there is clear evidence that the true spatial connections can be identified regardless of the length of the panel, long or short. Additional results presented in Online Appendix C, including those for models with $N = 50$ and $N = 100$, give further support to the effectiveness of two-stage VB.

We use high-performance computing (HPC) services for estimation. All computations are done using 1 compute node and 4 processor core. On average, each Monte Carlo

⁶We have also experimented on W_N , W_{N_1} and W_{N_2} of other forms. In addition, we have looked into models with different coefficients, $u_{t,1} \sim 0.1N(0, 1)$ and $u_{t,2} \sim 0.3N(0, 1)$. The Monte Carlo results provide further evidence that two-stage VB method works well. To save space, we do not report them in the paper.

replication for model (28) where $N = 30$ and $T = 80$ takes about 20 seconds, while for the same model, when $N = 30$ and $T = 20$ it takes about 60 seconds. For model (29), it again takes 20 seconds when $N = 30$ and $T = 80$. However, estimating model (29) takes 3 minutes when $N = 30$ and $T = 20$. The same pattern can be observed when estimating models where $N = 50$ and $N = 100$, that is: two-stage VB takes much longer to converge when $N \gg T$, and the larger the number of nonzero true parameters, the longer the estimation takes. To give a flavour of how fast two-stage VB converges, we would like to mention that, when allowing for parallel computing, each Monte Carlo replication of model (28) where $N = 100$ and $T = 50$ takes about 20 minutes, and that number reduces to 5 minutes for the same model where $N = 100$ and $T = 200$.

4 Empirical Applications

The relationship between sovereign bond ratings and spreads in eurozone countries is of great interest to researchers and policy makers alike, as explained in papers such as Gibson et al. (2021) and Hall et al. (*forthcoming*). One of the important questions posed is whether the spillovers of the southern euro area countries and their northern counterparts have different impacts on a member country, especially during the European debt crisis, also known as euro area crises, that started in late 2009 and lingered on well into 2015. Equally, it is important to know whether spillovers of a country group affect all the other countries differently. To answer those questions, we apply the two-stage VB approach on a sample containing five southern euro area countries – Spain, Greece, Ireland, Italy and Portugal – and five northern euro area countries – Austria, Belgium, France and Netherlands.

We use monthly data of Gibson et al. (2021). Sovereign rating is denoted by Rate, which is the combined sovereign ratings given by Standard and Poor’s, Fitch and Moody’s then transformed into numerical scale with ‘triple A’ having value 1 and ‘selected default’ having the value 22. Spread is defined as the difference between the yield on 10-year government bond of a country and that of Germany. Hence a rise in the rate or spread implies a worsening situation. Following Gibson et al. (2017), we use the following variables that capture the economic and political fundamentals as control variables: GDPgrowth, which is the real GDP growth rate; News, which

is fiscal news constructed using European Commission forecasts; $\frac{Debt}{GDP}$, which is the ratio of government debt to GDP; $\frac{CA}{GDP}$, which is the ratio of current account balance to GDP; $\frac{P}{P^*}$, which is the ratio of a country's harmonised consumer price to that of Germany; and Pol , which is the index of political uncertainty reflecting the climate for foreign investors and political uncertainty. The monthly data runs from January 2000 to April 2019. For brevity, we report the data sources in the Appendix.

Taking account of the feedback loop between sovereign bond ratings and sovereign spreads, our model takes the following form:

$$\begin{aligned}
Rate_{it} = & c_{11,i} + c_{12,i} * Spread_{it} + c_{13,i} * GDPgrowth_{it} + c_{14,i} * \frac{Debt_{it}}{GDP_{it}} + c_{15,i} * News + \\
& c_{16,i} * \frac{P}{P^*}_{it} + c_{17,i} * Rate_{i(t-1)} + W_i^{rate} * Rate_t + \varepsilon_{it}^{rate} \\
Spread_{it} = & c_{21,i} + c_{22,i} * Rate_{it} + c_{23,i} * GDPgrowth_{it} + c_{24,i} * \frac{Debt_{it}}{GDP_{it}} + c_{25,i} * Pol_{it} + \\
& c_{26,i} * \frac{CA_{it}}{GDP_{it}} + c_{27,i} * Spread_{i(t-1)} + W_i^{sp} * Spread_t + \varepsilon_{it}^{sp}
\end{aligned} \tag{30}$$

where $Rate_t = (Rate_{1t}, \dots, Rate_{10t})'$ and $Spread_t = (Spread_{1t}, \dots, Spread_{10t})'$. Note that W_i^{rate} and W_i^{spread} are the i^{th} row of the 10×10 spatial weights matrices W^{rate} and W^{spread} , respectively. Note that W^{rate} and W^{spread} are both with zero diagonals and the rest of the elements to be estimated.

To trace how the spillovers fluctuate over time, we use window sizes of 24, 36, 60 and 120 months, respectively, for the rolling window estimations. For the i^{th} country, the average rating spatial spillovers from the south is computed by taking the mean of the non-zero elements in W_i^{rate} that are associated with the southern euro area countries; and the average rating spatial spillovers from the north is computed by taking the mean of the non-zero elements in W_i^{rate} that are associated with the northern euro area countries. In the same fashion, we calculate the average spread spatial spillovers from the south and the north. To put the values in context, if the ratings of n countries each increases by 1 notch value, the rating of country i , which is not included in those countries, would increase by n notches timing the average rating spillovers calculated for the n countries; Likewise, if the spreads of the n countries each increases by 1 basis point, the spread of country i would increase by n basis points timing the average

spreads spillovers calculated for the n countries.⁷

Figures 1-4 present the average spatial spillovers from the southern euro area countries and those from the north using different window sizes. Two salient patterns leap directly from the graphs. First, the rating spillovers tend to remain unchanged over time for data of various rolling windows while the spread spillovers vary all the time. This is not surprising because there are a lot of volatilities in the sovereign spreads data while the sovereign ratings only take a relatively small number of step-wise changes. Second, despite the plots for longer windows are relatively smoother and with smaller magnitudes in comparison with plots for shorter windows, average spillover plots of the same country tend to convey very similar, or even the same, information, which we will next go into details about.

Let us start with the impacts of rating spillovers on a northern euro area country. Observe an average increase in rates from the southern countries tends to worsen the sovereign rating of a northern country, except France, especially during the period of Euro area crises. For France, the picture is exactly the opposite. For a northern country, an average increase in rates in the rest of northern countries, however, has mixed effects on itself: it tends to worsen the ratings of Austria and France (causing the values of their rates to increase), while improve the ratings of Belgium, Finland and Netherland (causing their rates to decrease).

For a southern country, apart from Greece, an average increase in rates of the northern countries tends to worsen its ratings. For Greece, especially in the euro area crises, there is strong evidence that its sovereign ratings move in the opposite directions of northern countries's ratings. Put it another way, an improvement in the ratings of northern countries is usually associated with a deterioration in Greek sovereign ratings. The impacts of an average increase in rates of the southern countries are more mixed: Before the euro area crises, that increase tends to worsen a southern country's rating; In and after the crises, it by contrast tends to improve a southern country's ratings.

⁷Technically, our method can untangle the spillover behaviours further, say tracking the spillover effects of one country on another. In this paper, we focus on comparing and contrasting the impacts of spillovers of the southern euro area countries and their northern counterparts for the issue's greater research interest.

For a northern country, the messages from the spread spillovers is divided by 2007, the global financial crises. Before 2007, the pictures are quite mixed. From 2007, an average increase in the spreads of other northern countries is always associated with an increase in its own spread, making it more costly for the country to borrow. In the same period, an increase in the spreads of southern countries tends to be associated with an increase in the spread of a northern country too. But the magnitude of the latter is barely minimum in comparison to that of the former. It is remarkable that 2007 plays such an important role here while the influence of euro area crises is almost not distinguishable.

For a southern country, the situation of spread spillovers is more complicated. When the sample size is large enough, say setting the window size to be 10 years, we observe that for most of the time an average increase in the spreads in southern countries has a much larger positive impact on a southern country's spread than an average increase in the spreads in northern countries does, for Spain, Greece, Italy and Portugal. For Ireland though, the effects of an increase in northern countries' spread is larger than that of the southern countries. When we reduce the window sizes, the prominence of the euro area crisis period becomes more obvious. For example, using rolling window of 5 years, we observe that, from 2005 onwards, when there is an average increase in the spreads of southern countries or an average decrease in the spreads of northern countries, the spreads of Greece, Ireland and Italy would go up. While for Spain and Portugal, especially from 2007 to 2012, both an average increase in the spreads of the northern countries and an average increase in the spreads of the southern countries are associated with an increase in the spreads in their own country, with the former of a much larger magnitude than the latter. This implies that the sovereign debt market was treating Greece, Ireland and Italy in a very different manner from the way it treated Spain and Portugal. Yet, that 'honeymoon period' for Spain and Portugal didn't last long: Since 2012, they have joint the rest of the southern countries in the sense that their spreads would increase if there is an average increase in the southern countries' spreads or an average decrease in the northern countries' spreads.

5 Conclusions

In applied work, if the spatial weights matrix set a priori were to be far from its true value, the empirical analysis using SAR models would be misleading. In this paper, we have developed a two-stage VB approach to estimating panel SAR models with unknown spatial weights matrices so as to let the data speak. Our two-stage VB with D-L priors method can be easily extended by using other popular priors such as the Lasso, Horseshoe and spike and a slab priors. Furthermore, the success of two-stage VB shows the potential of combining VB with more sophisticated methods, such as three-stage least squares, full information likelihood and GMM to estimate panel SAR models, especially those involving $N \gg T$. Monte Carlo experiments show that our two-stage VB is rather fast, and it can recover the spatial impacts well for both the long and short panels.

As an empirical example, we apply the two-stage VB to the sovereign bond ratings and sovereign spreads data of 10 eurozone countries to uncover the impacts of spatial spillovers of the southern countries, which were more severely hit by the eurozone crises, and those of the northern countries. Without pre-imposing any spatial weights matrices that might be unrealistic, we are able to shed new lights on the spillover behaviours of the south and the north. To our best knowledge, our findings are among the first in the literature to delineate how an individual country is affected by the spillovers from other countries in the eurozone.

References

- [1] Ahrens, A., and A. Bhattacharjee (2015). Two-step lasso estimation of the spatial weights matrix. *Econometrics*, 3, 128–155.
- [2] Anselin, L. (1988). *Spatial Econometrics: Methods and Models*. Kluwer Academic, Dordrecht.
- [3] Baltagi, B., S.H. Song and W. Koh (2003). Testing panel data regression models with spatial error correlation. *Journal of Econometrics*, 117, 123–150

- [4] Baltagi, B. H., P. Egger and M. Pfaffermayr (2013). A generalized spatial panel data model with random effects. *Econometric Reviews*, 32(5-6), 650-685.
- [5] Basak, G. K., A. Bhattacharjee and S. Das (2018). Causal ordering and inference on acyclic networks. *Empirical Economics*, 55, 213–232.
- [6] Bhattacharya A., D. Pati, N. S. Pillai and D. B. Dunson (2015). Dirichlet–Laplace priors for optimal shrinkage. *Journal of the American Statistical Association*, 110 (512), 1479-1490
- [7] Blei, D.M., A. Kucukelbir and J.D. McAuliffe (2017) Variational inference: A review for statisticians. *Journal of the American Statistical Association*, 112 (518), 859-877.
- [8] Case, A. (1991). Spatial Patterns in Household Demand. *Econometrica*, 59, 953-965.
- [9] Cliff, A. D. and J. K. Ord. (1973). *Spatial Autocorrelation*. London: Pion.
- [10] Fox, J. (1979). Simultaneous equation models and two-stage least squares. *Sociological methodology*, 10, 130-150.
- [11] Gibson, H. D., S. G. Hall and G. S. Tavlás (2017). Self-fulfilling dynamics: The interactions of sovereign spreads, sovereign ratings and bank ratings during the euro financial crisis. *Journal of International Money and Finance*, 73, 371-385.
- [12] Gibson, H. D., S. G. Hall, D. GeFang, P. Petroulas and G. S. Tavlás (2021). Cross-country spillovers of national financial markets and the effectiveness of ECB policies during the euro-area crisis. *Oxford Economic Papers*, 73(4), 1454-1470.
- [13] Gefang, D., G. Koop and A. Poon (2020). Computationally efficient inference in large Bayesian mixed frequency VARs. *Economics Letters*, 191, 109120.
- [14] Gefang, D., G. Koop and A. Poon (2022). Forecasting using variational Bayesian inference in large vector autoregressions with hierarchical shrinkage. *Interna-*

tional Journal of Forecasting.

- [15] Hall, S. G., D. Gefang and G. S. Tavlás (forthcoming). A test to select between spatial weighting matrices. *Journal of Spatial Econometrics*.
- [16] Krock, M., W. Kleiber and S. Becker (2021). Nonstationary modeling with sparsity for spatial data via the basis graphical lasso. *Journal of Computational and Graphical Statistics*, 30(2), 375-389.
- [17] Lam, C., and Souza, P. C. (2019). Estimation and selection of spatial weight matrix in a spatial lag model. *Journal of Business and Economic Statistics*, 38, 693–710.
- [18] Lee, L-F. and J. Yu (2010). Estimation of spatial autoregressive panel data models with fixed effects. *Journal of Econometrics*, 154, 2, 165-185.
- [19] Li, Y., B. A. Craig and A. Bhadra (2019). The graphical horseshoe estimator for inverse covariance matrices. *Journal of Computational and Graphical Statistics*, 28(3), 747-757.
- [20] Liu, X. and P. Saraiva (2019). GMM estimation of spatial autoregressive models in a system of simultaneous equations with heteroskedasticity. *Econometric Reviews*, 38:4, 359-385.
- [21] Loaiza-Maya, R., M. S. Smith, D. J. Nott and P. J. Danaher (2021). Fast and accurate variational inference for models with many latent variables. *Journal of Econometrics*.
- [22] Makalic, E. and D. F. Schmidt (2016). A simple sampler for the horseshoe estimator. *IEEE Signal Processing Letters* 23, 179–182.
- [23] Ormerod, J.T. and M. P. Wand (2010). Explaining variational approximations. *The American Statistician*, 64 (2), 140-153.
- [24] Tibshirani, R. (1996). Regression shrinkage and selection via the lasso. *Journal of the Royal Statistical Society, Series B*, 58, 267-288.

- [25] Wang, H. (2012). Bayesian graphical lasso models and efficient posterior computation. *Bayesian Analysis*, 7(4), 867-886.
- [26] Yang, K. and L. F. Lee (2017). Identification and QML estimation of multivariate and simultaneous equations spatial autoregressive models. *Journal of Econometrics* 196:196–214.
- [27] Zellner, A., and H. Theil (1962). Three-Stage Least Squares: Simultaneous Estimation of Simultaneous Equations. *Econometrica: Journal of the Econometric Society*, 54-78.

Appendix: Data Sources

- Spreads: monthly data from Statistical Data Warehouse, European Central Bank
- Ratings: monthly data from Fitch, Standard and Poor's and Moody's
- The ratio of government debt to GDP: quarterly data from Thomson Reuters Datastream
- Real GDP growth: quarterly data from Thomson Reuters Datastream
- Current account balance as a percentage of GDP: Either monthly or quarterly data from Thomson Reuters Datastream
- Harmonised Consumer Price Index: monthly data from Thomson Reuters Datastream
- Political uncertainty: quarterly data from IFO World Economic Survey. Two variables have been used in order to create the variable political uncertainty. 1) The present climate for foreign investors, political stability (which was discontinued), which was updated with information from the new variable, 2) Political instability, using an appropriate mapping for the reported values of each variable.

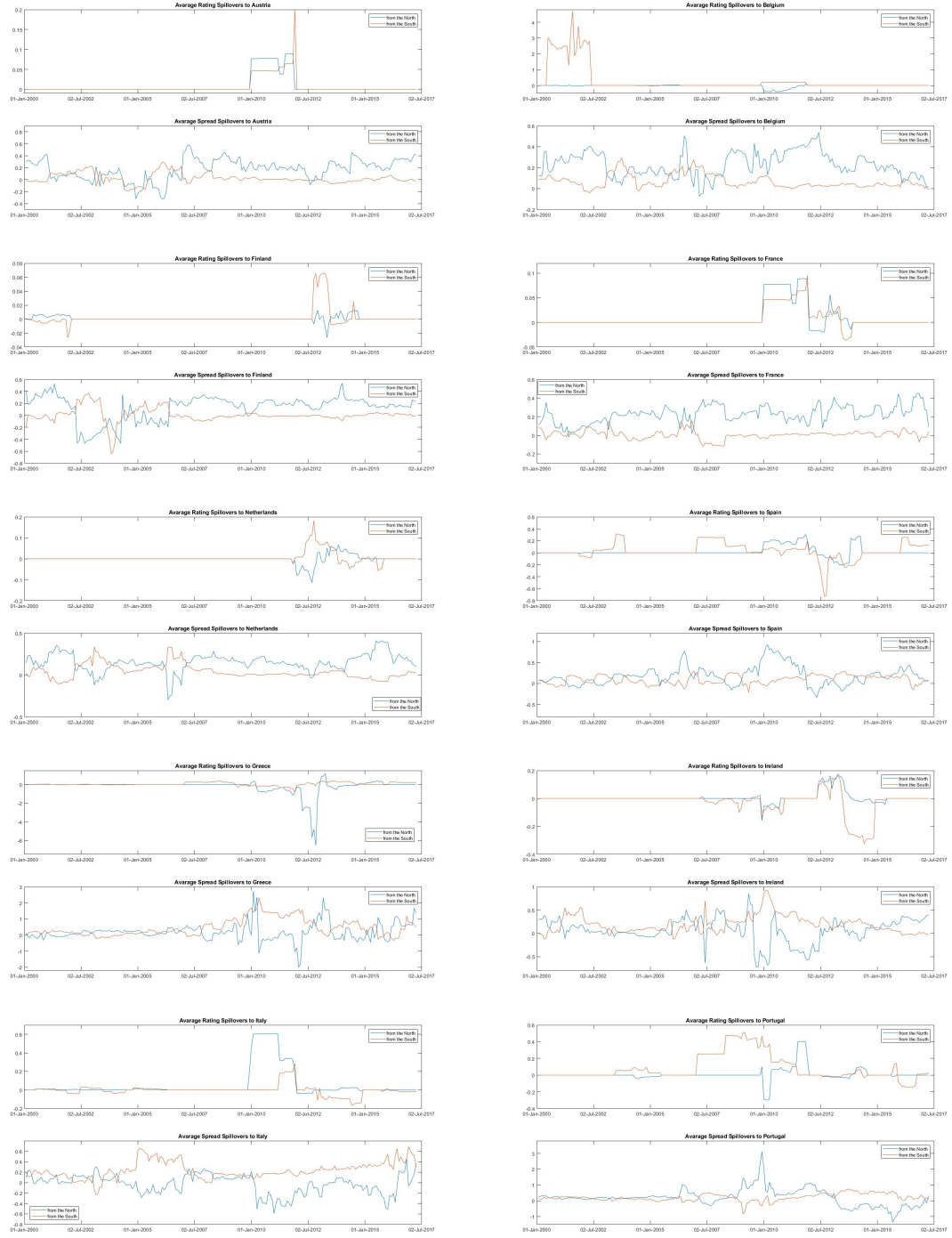


Figure 1: Rolling Window of 24 Months

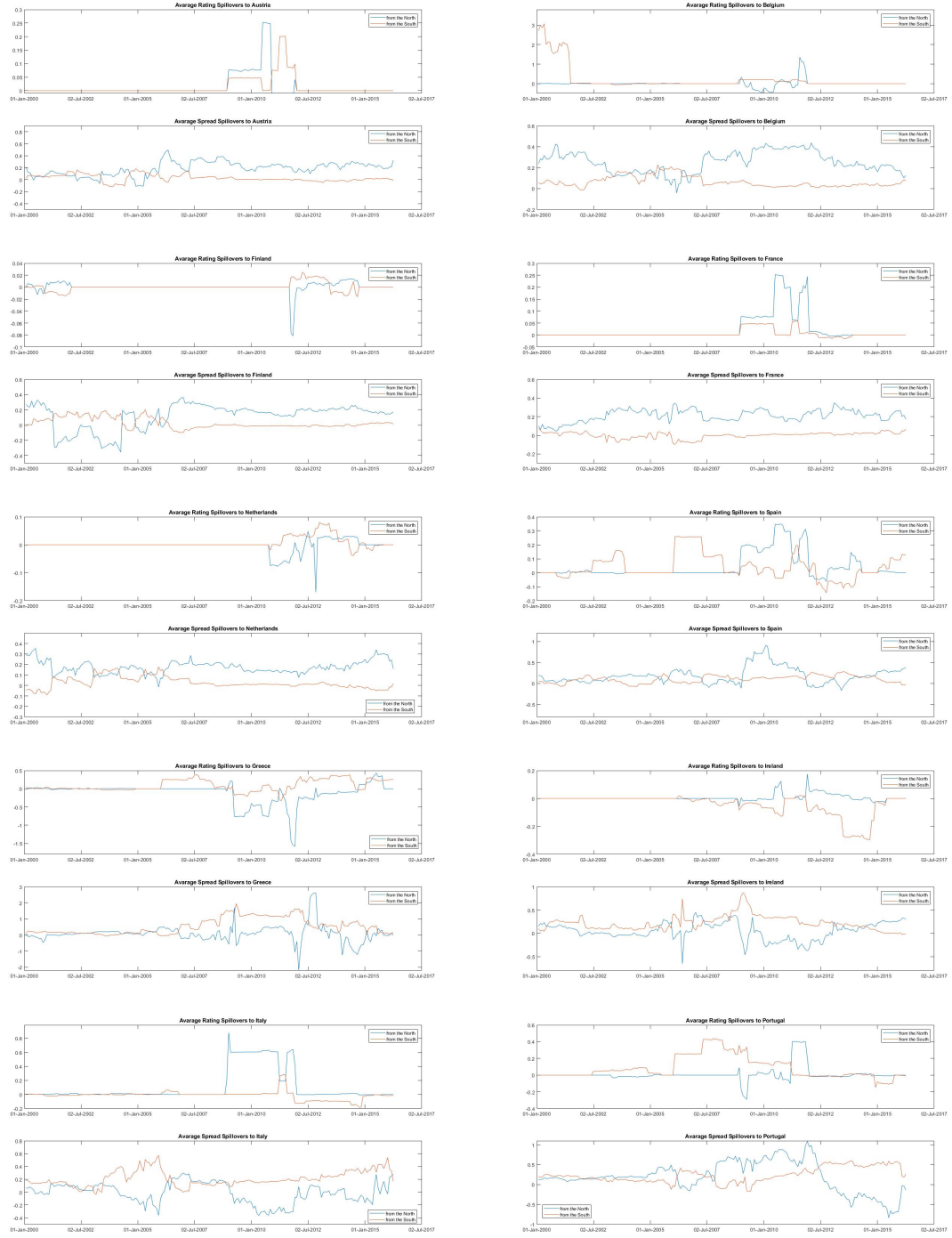


Figure 2: Rolling Window of 36 Months

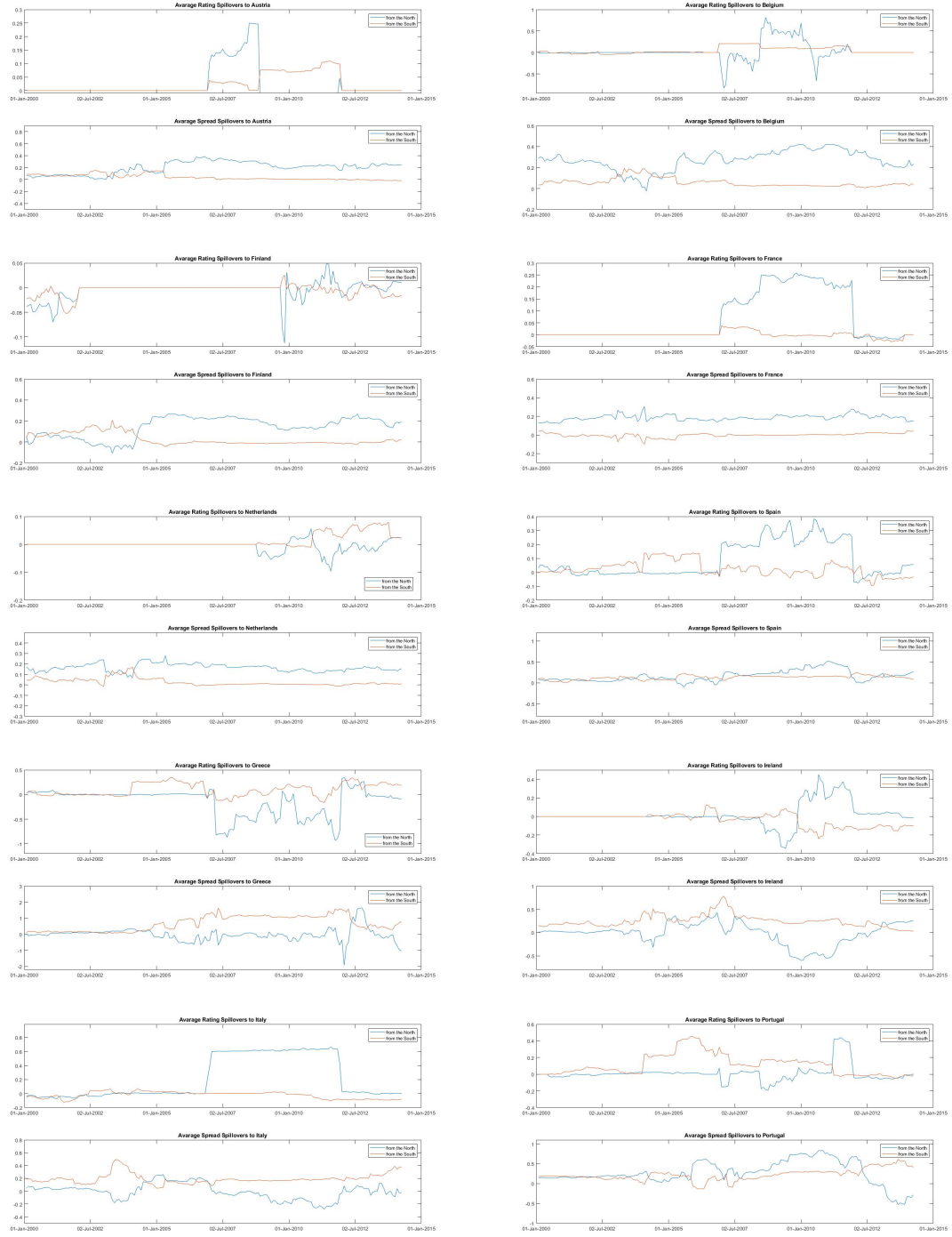


Figure 3: Rolling Window of 60 Months

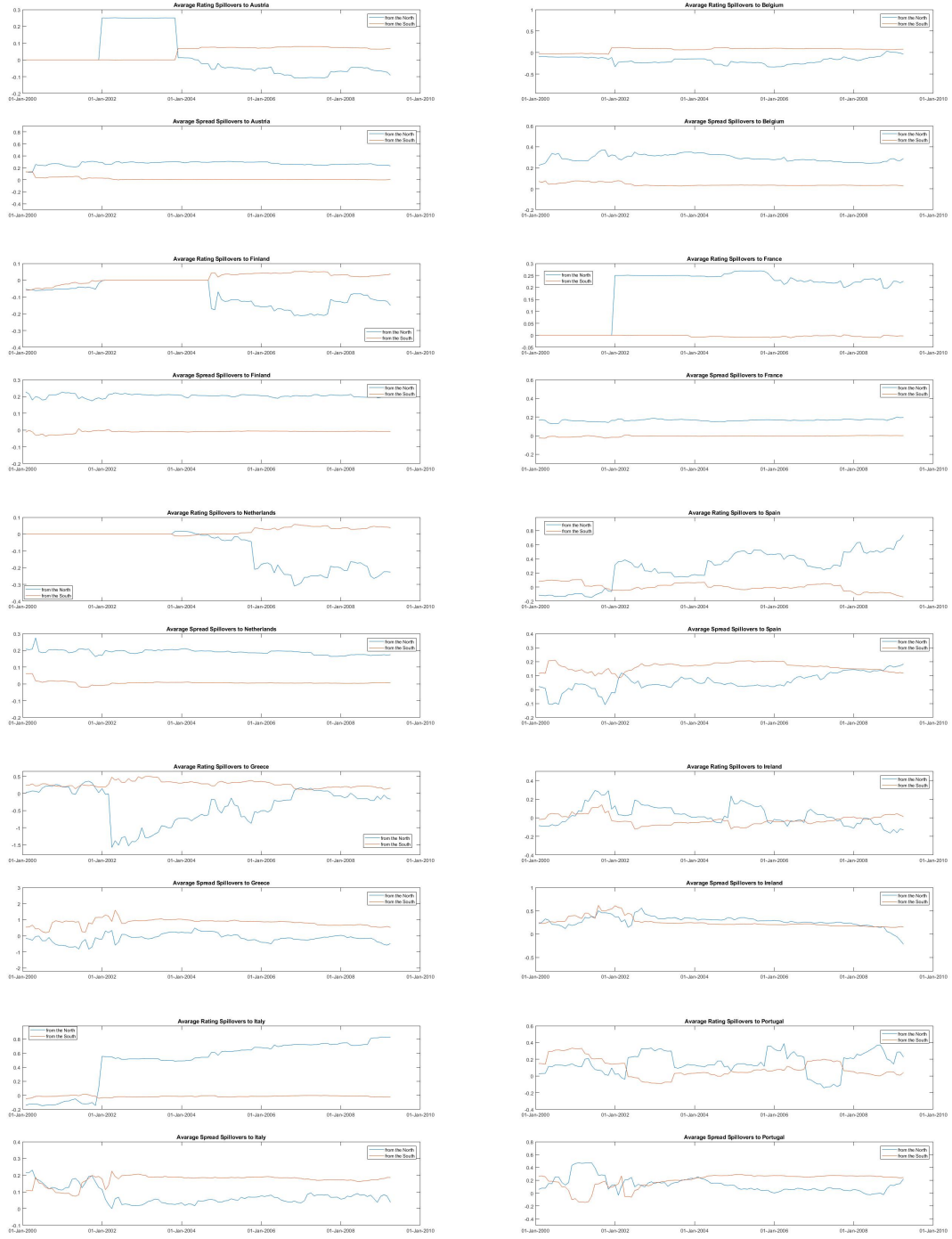


Figure 4: Rolling Window of 120 Months

